Heliyon 10 (2024) e34611

Contents lists available at ScienceDirect

Heliyon

journal homepage: www.cell.com/heliyon

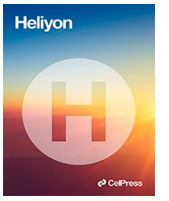

Research article

A novel highly sensitive inner filter effect-based fluorescence immunoassay with quantum dots for bioanalysis of zolbetuximab, a monoclonal antibody used for immunotherapy of gastric and gastroesophageal junction adenocarcinoma

Ibrahim A. Darwish [a,*], Daohong Zhang [b], Mohammed S. Alsalhi [a]

[a] Department of Pharmaceutical Chemistry, College of Pharmacy, King Saud University, P.O. Box 2457, Riyadh, 11451, Saudi Arabia
[b] College of Food Engineering, Bio-Nanotechnology Research Institute, Ludong University, Yantai, 264025, Shandong, China

ARTICLE INFO

Keywords:
Gastric/gastroesophageal adenocarcinoma
Immunotherapy
Zolbetuximab
Fluorescence immunoassay
Inner filter effect
Quantum dots

ABSTRACT

Zolbetuximab (ZOL) is a groundbreaking monoclonal antibody targeting CLDN 18.2, a cancer cell surface protein. It is a first-in-class therapy for gastric and gastroesophageal junction adenocarcinoma. However, there is currently any immunoassay available for bioanalysis of ZOL, hindering its pharmacokinetic studies, therapeutic monitoring, and safety profile refinement. To address this gap, this study presents the development and validation of a novel highly sensitive inner filter effect-based fluorescence immunoassay (IFE-FIA) with quantum dots (QDs) as a probe. This assay enables the quantitative determination of ZOL in plasma samples. The assay involved non-competitive capturing of ZOL from the samples using a specific antigen (CLDN 18.2 protein) immobilized on assay plate microwells. A horseradish peroxidase (HRP)-labelled anti-human IgG was used to measure the immune complex. The assay's detection system relies on the formation of a light-absorbing colored product through an HRP-catalyzed oxidative reaction with the substrate 3,3′,5,5′-tetramethylbenzidine. This light absorption efficiently quenched the fluorescence of QDs via the IFE. The measured fluorescence signals corresponded to the concentrations of ZOL in the samples. The conditions of the IFE-FIA and its detection system were refined, and the optimum procedures were established. Following the guidelines of immunoassay validation for bioanalysis, the assay was validated, and all the validation criteria were acceptable. The assay demonstrates high sensitivity, accurately quantifying ZOL at concentrations as low as 10 ng/mL in plasma samples, with acceptable precision. Importantly, it avoids interferences from endogenous substances and plasma matrix. The recoveries in spiked human plasma ranged from 96.8 % to 104.5 %, with relative standard deviations of 4.1 %–6.5 %. The proposed IFE-FIA represents a valuable tool for quantifying ZOL in clinical settings, enabling assessment of its pharmacokinetics, therapeutic drug monitoring, and safety profile refinement.

1. Introduction

The gastric and gastroesophageal junction (G/GEJ) adenocarcinoma is a highly aggressive malignant tumor that has been showing

* Corresponding author.
E-mail address: idarwish@ksu.edu.sa (I.A. Darwish).

https://doi.org/10.1016/j.heliyon.2024.e34611
Received 5 February 2024; Received in revised form 11 June 2024; Accepted 12 July 2024
Available online 14 July 2024

a substantial increasing occurrence over the years. This poses a significant threat to human health and imposes substantial financial burdens on society. Surgical intervention is commonly employed for the effective treatment of resectable G/GEJ adenocarcinoma. However, most patients experience early local recurrence or distant metastasis after surgery. The treatment of advanced metastatic G/GEJ adenocarcinoma with a dismal prognosis is challenging and the median overall survival ranged from 9 to 14 months [1–5]. Currently, the first-line standard treatment is determined based on three molecular characteristics: HER2-positive, HER2-negative, and dMMR/MSI-H. The use of anti-HER2-targeted therapy and immunotherapy has significantly improved the survival rates of patients with HER2-positive tumors and high PD-L1 expression in gastric cancer [4,5]. However, HER2-negative patients with low PD-L1 expression face difficulties in benefiting from these treatment approaches, leaving chemotherapy as the limited option, which is not effective in controlling the disease [6,7]. Abnormal changes in claudin, a protein involved in tight junctions, are associated with impaired tight adhesion and disruption of epithelial cell polarity. These structural abnormalities contribute to increased cell proliferation, epithelial-mesenchymal transition, invasion, and metastasis [8–10].

Despite the significant progress made in systemic treatment in recent years, there remains a substantial unmet need in the field. As the field of tumor therapy gradually shifts towards the era of macromolecular medicine, the focus of new drug research and development has turned to the selection of targets such as Claudin 18.2 (CLDN 18.2). Research studies have demonstrated that gastric cancers with positive CLDN 18.2 expression, defined as having more than 40 % of tumor cells showing immunohistochemical staining intensity $\geq$2+, account for approximately 49 %–85 % of all gastric cancers [11–13]. Furthermore, high CLDN 18.2 expression is observed in approximately 24 %–36 % of gastric cancers [14,15]. Given its specificity and high expression in gastric cancer patients, CLDN 18.2 has emerged as a promising target for the development of new drugs for gastric cancer, offering a new direction for targeted therapy in this disease.

Zolbetuximab (ZOL, previously known as IMAB362) is a groundbreaking chimeric lgG1 humanized monoclonal antibody that represents a "first-in-class" treatment targeting CLDN 18.2 [16,17] for the treatment of patients with HER2-negative CLDN 18.2 strongly positive locally advanced unresectable or metastatic G/GEJ adenocarcinoma. ZOL was developed by Qure Biotechnology Co., Ltd. (Shanghai, China). Several recent studies have demonstrated that first-line treatment with ZOL plus chemotherapy can improve prognosis in patients with advanced G/GEJ adenocarcinoma [18–20]. ZOL exerts its antitumor effects through antigen-specific activation of immune effector mechanisms and induces both antibody-dependent cell-mediated cytotoxicity and complement-dependent cytotoxicity [21,22]. The recent data confirmed the excellent anti-tumor activity of ZOL, which can reduce the risk of death similarly in the SPOTLIGHT [19] and GLOW [20] trials. Based on these promising findings, the Food and Drug Administration (FDA), On July 10, 2023, accepted and granted a priority review for a biologics license application regarding ZOL for first-line treatment of locally advanced unresectable or metastaticHER2-negative G/GEJ adenocarcinoma with CLDN18.2-positive tumors [23]. However, the information about its pharmacokinetic properties, ways of therapeutic monitoring, and safety profile is very limited [24]. To support the pharmacokinetic studies, therapeutic monitoring, and refine the safety profile of ZOL, an efficient analytical tool is seriously needed. Based on extensive literature survey, up to date, there has been no published method for the quantification of ZOL in a biological matrix such as plasma. The present study describes, for the first time, the development and validation of a highly sensitive and reliable inner filter effect-based fluorescence immunoassay (IFE-FIA) with quantum dots (QDs) as a probe for the quantitation of ZOL in human plasma.

The relevance and significance of ZOL concentration monitoring in human plasma are highlighted in the following points: (1) Therapeutic efficacy because monitoring ZOL concentrations can provide valuable insights into the drug's therapeutic efficacy. By assessing the drug levels over time, clinicians can optimize the dosage and treatment regimen to ensure adequate drug exposure. This information can help maximize treatment outcomes and minimize the risk of under- or over-dosing. (2) Pharmacokinetic studies as the understanding the pharmacokinetics of ZOL is essential for optimizing its dosing and administration. Monitoring ZOL concentrations enables the assessment of drug absorption, distribution, metabolism, and elimination. This information can guide dosing strategies, especially in patients with altered pharmacokinetics due to factors such as age, comorbidities, or concomitant medications. (3) Safety and toxicity as the monitoring ZOL concentrations can aid in evaluating the drug's safety profile. By correlating drug concentrations with adverse events, clinicians can identify potential toxicity and implement appropriate measures to mitigate risks. This information is particularly relevant in patients with known risk factors or those undergoing long-term ZOL therapy. (4) Therapeutic drug monitoring which allows individualized dosing based on a patient's specific drug metabolism and response, leading to improved therapeutic efficacy and reduced toxicity. (5) Research and development because monitoring ZOL concentrations contributes to ongoing research and development efforts. By obtaining comprehensive pharmacokinetic data, researchers can refine dosing regimens, explore potential drug interactions, and uncover factors influencing treatment outcomes. This knowledge can guide future advancements in ZOL-based therapies.

The strategy involved in the development of IFE-FIA is summarized in the following points. Immunoassays such as enzyme-linked immunosorbent assays (ELISAs) are mostly recommended for the quantitation of therapeutic monoclonal antibodies in biological matrices. This recommendation is due to their specificity, sensitivity, cost-effectiveness, and suitability for large-scale screening in clinical settings [25–28]. These ELISAs have been mostly developed using commercial immobilized anti-idiotype antibodies for capturing the analytes; however, this approach might lead to false positive results due to the non-specific binding of similar human IgG antibodies in the samples and provide moderate sensitivity [29]. Fluorescence immunoassays (FIAs) have been proposed as a better alternative for ELISAs [30]. The FIAs offered simpler operational procedures, a wider range, higher sensitivity, and better accuracy and precision than ELISAs do.

Quantum dots (QDs) have been introduced with unique advantages, such as large Stokes shift, good optical stability, high quantum yield and adjustable emission wavelength [31–33]. These advantages were behind the employment of QDs as fluorescence probes in the development of highly sensitive FIAs for different targets [34–36]. A higher sensitivity of QDs-based FIA could be obtained if a

fluorescence signal readout is combined with an enzymatic reaction for the detection system of FIA. Therefore, the present study undertook the commitment to develop an FIA for ZOL with a detection system comprising QDs and an enzyme reaction. In the detection system described herein, fluorescent QDs were used as a signal probe, and an enzymatic color-forming enzymatic reaction of HRP/TMB was used to quench the fluorescence of QDs through the IFE. In this assay (IFE-FIA), the concentrations of ZOL in its sample solutions were quantified based on their direct relation with the degree of QDs fluorescence inhibition.

2. Experimental

2.1. Instruments

Spectramax M5 (Molecular Devices, California, USA) multifunctional (absorbance, fluorescence, chemiluminescence) microplate/cuvette reader was used for scanning the fluorescence spectra and conducting the IFE-FIA procedures. Automatic microplate strip washer (ELx 50: Bio-Tek Instruments Inc., Winooski, USA). Incubator (MINI/18: Genlab Ltd, Widnes, UK). A double-beam ultraviolet–visible spectrophotometer (V-530: JASCO Co. Ltd., Kyoto, Japan). Microprocessor laboratory pH meter (BT-500: Boeco, Hamburg, Germany). Ultrasonic sonicator cleaning system (X-TRA150H: Elma, England). Vortex (Clifton cyclone CM1: Weston, England). Refrigerated centrifuge (1-15 PK: Sigma Laborzentrifugen GmbH, Osterode, Germany). Electric digital balance (JB1603-C/FACT: Mettler-Toledo International Inc., Zürich, Switzerland). Water purification system (Purelab Flex: Elga Veolia Ltd, High Wycombe, UK).

2.2. Materials

Reference standard material of ZOL (IMAB362) with a purity of 96.98 % was purchased from MCE MedChem Express (New Jersey, NJ, USA). CLDN 18.2 protein was purchased from Arco Biosystems (Newark, DE, USA). Goat anti-human HRP-IgG conjugate and bovine serum albumin (BSA), Tween 20, 3,3′,5,5′-tetramethylbenzidine (TMB) substrate solution, and QDs (CdSe/ZnS core-shell type quantum dots with quantum yield $\geq$50 %) were purchased from Sigma-Aldrich Chemicals Co. (St. Louis, Missouri, USA). White opaque flat-bottom high binding 96-well plates for FIA were purchased from Corning Ltd. (New York, NY, USA). Human plasma samples were provided by the King Khalid Hospital of King Saud University (Riyadh, Saudi Arabia). The samples were stored frozen at −20 °C until they were utilized in the experiment. All other chemical/reagents and buffer components used throughout the work were of analytical grade.

2.3. Preparation of solutions

2.3.1. Solutions of ZOL antibody and CLDN 18.2 protein

The stock solutions (1 mg/mL) of ZOL and CLDN 18.2 were prepared by dissolving 5 mg of the substance in 5 mL of phosphate-buffered saline (PBS, pH 7.4) and carbonate buffer (CB, pH 9.6), respectively. This stock solution was further diluted with the same corresponding buffer solution to yield working solutions of suitable concentrations for the corresponding experiment. The stock solutions of ZOL and CLDN 18.2 were kept at −20 °C and the working solutions were kept at 4 °C until use.

2.3.2. IFE-based fluorescence quenching solution

The IFE-based fluorescence quenching solution was freshly prepared by mixing TMB HRP substrate solution with QDs in a ratio of 80:20 (v/v).

2.4. Procedures of IFE-FIA

The 96-well flat-bottom FIA plates were coated with 50 μL of CLDN 18.2 protein (1 μg/mL, in CB, pH 9.6) by incubation the plates containing the CLDN 18.2 protein solutions at 37 °C for 2 h. The coating solution was removed from the plate wells by washing the plates 3 times with a washing buffer (PBS-T: PBS containing Tween 20 at a concentration of 0.5 %, v/v). The plate wells were blocked by 100 μL of BSA solution (2 %, w/v, in PBS) by incubation the plates at 37 °C for 1 h, followed by washing with PBS-T. Aliquots (50 μL) of ZOL solutions (standards, quality control samples, or plasma samples) were dispensed into the wells of coated and blocked assay plates. The plates were incubated at 37 °C for 1 h, followed by washing. During this incubation step, ZOL in the samples was captured by the immobilized CLDN 18.2. An aliquot (50 μL) of HRP-IgG (0.5 μg/mL, in PBS) was added and the plates were incubated at 37 °C for 1 h, followed by a washing step. An aliquot (100 μL) of IFE-based fluorescence quenching solution was added to the wells. The plates were incubated at 37 °C for 15 min, and the fluorescence intensity was measured by the microplate reader at 340/525 nm for excitation/emission, respectively. The measured fluorescence intensities of standard solutions of ZOL were related to the corresponding ZOL concentration to generate the calibration curve. From the calibration curve, the ZOL concentrations in plasma samples were computed.

2.5. Validation experiments of IFE-FIA procedures

2.5.1. Calibration and quantitation range

The experiment involved the use of calibration ZOL solutions in PBS. The concentrations of calibration solutions were in the range

of 2–5000 ng/mL. The working quantitation range of the assay was defined as the concentration range which gave an inhibition of the maximum fluorescence intensity (presented as ΔF) in the range of 10–90 %. The concentrations that gave 10 % and 20 % fluorescence inhibition were defined as the lower limit of quantitation (LLOQ) and upper limit of quantitation (ULOQ), respectively.

2.5.2. Accuracy and precision

The intra- and inter-assay accuracy and precision of the IFE-FIA were assessed by analysis of ZOL-containing samples at three different concentration levels. For the intra-assay experiment, 3 replicates of each sample were analyzed, as a batch, in a single assay run. For the inter-assay experiments, triplicates of each sample were analyzed on two consecutive days. The accuracy and precision were expressed as recovery and relative standard deviations (RSD), respectively. The recovery values were calculated using the formula: recovery (%) = (measured ZOL concentration/nominated ZOL concentration) × 100.

2.5.3. Plasma matrix effect

The plasma matrix effect experiment was conducted using 3 replicates of plasma samples spiked with ZOL and diluted with PBS. Blank plasma samples were spiked with ZOL to yield a concentration of 400 ng/mL. These samples were then serially diluted in PBS to yield concentrations within the working range of the IEF-FIA (10–400 ng/mL). These diluted samples were analyzed by the IFE-FIA and the recovery values of the nominated ZOL concentrations and RSD values were calculated.

3. Results and discussion

3.1. Assay description and design

Fig. 1 illustrates the characteristics and technical steps of the proposed IFE-FIA. In this assay, the capturing antigen (CLDN 18.2 protein) was immobilized onto the inner surfaces of microwells of assay plates (Fig. 1A). Subsequently, ZOL-containing samples were added, and the plates were incubated to enable the ZOL molecules in the samples to be captured by the immobilized CLDN 18.2 protein (Fig. 1B). An anti-human HRP-IgG antibody was allowed to bind to the complex (CLDN 18.2-ZOL) formed onto the plate wells

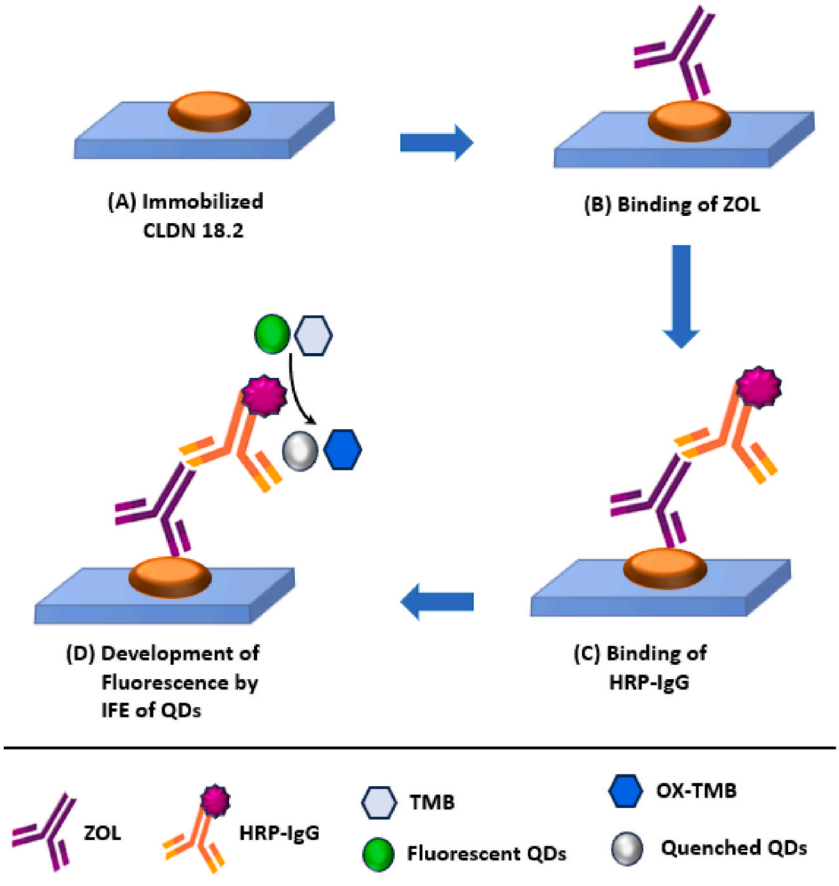

Fig. 1. A schematic diagram for the IFE-FIA for the quantitation of ZOL by employment of IFE of QDs on the chromogenic HRP-catalyzed oxidation of TMB for detection system.

(Fig. 1C). The IFE-based fluorescence quenching solution containing the HRP chromogenic substrate (TMB) and QDs were added, and the reaction was allowed to proceed (Fig. 1D). During the reaction, colorless TMB molecules were transformed by the HRP-catalyzed oxidative reaction into the corresponding blue colored oxidized TMB molecules (OX-TMB). The absorbance of these colored molecules quenched the QDs fluorescence. The degree of fluorescence quenching (ΔF) was related to the HRP molecules bound to the CLDN 18.2-ZOL complex, and accordingly to the ZOL concentration in its sample.

CLDN 18.2 protein was selected as a capturing reagent in the IFE-FIA because CLDN 18.2 protein is specifically targeted by ZOL antibody [16,17]. Various assay formats could be adapted for the development of IFE-FIA but the direct non-competitive binding format was chosen because it usually provides high accuracy and precision at low analyte concentrations and overall simplicity with a relatively short assay time [37,38]. White-opaque 96-microwell plates were chosen for the IFE-FIA as they have been shown to provide the highest fluorescence intensity, sensitivity, and precision compared to black-opaque and transparent plates [39]. Since ZOL is an IgG subtype antibody, an anti-human IgG antibody conjugated to HRP was utilized to detect ZOL bound to the immobilized CLDN 18.2. The IFE of HRP/TMB enzymatic reaction on the fluorescence of QDs was employed to simplifies the procedures, avoid the chemical labelling with a fluorescent probe, and eliminates the possible loss of immunoreactivity of the second antibody upon its labelling.

3.2. Assessment of the IFE between HRP/TMB and QDs

The IFE phenomenon has attracted scientific researchers' interest as a simple, effective, and convenient fluorescence burst mechanism, and has been applied in various immunoassays [40,41]. In the IFE process, a light-absorbing molecule in a solution absorbs the excitation or emission wavelength of a fluorescent probe in the solution, resulting in a decrease in the fluorescence intensity of the probe. It is a non-irradiated energy conversion process and does not require complex labelling processes. The specific interaction distance between the fluorescence donor and acceptor (light absorbent) is not a consideration, making it an effective and powerful technique for developing novel fluorescence assays [42]. In this study, the interaction between QDs fluorescence and OX-TMB light absorption was investigated by UV–visible spectrophotometry. It was found that the absorption peak of OX-TMB at 370 nm overlaps with the excitation wavelength of QDs at 340 nm, and the high molar absorptivity of OX-TMB allows its absorption for the excitation light of QDs (Fig. 2A). This ensures the occurrence of IFE process [43]. The detailed effect of TMB on the fluorescence of QDs has indeed been studied in a previous investigation [34]. The interference and background fluorescence were also investigated, as they

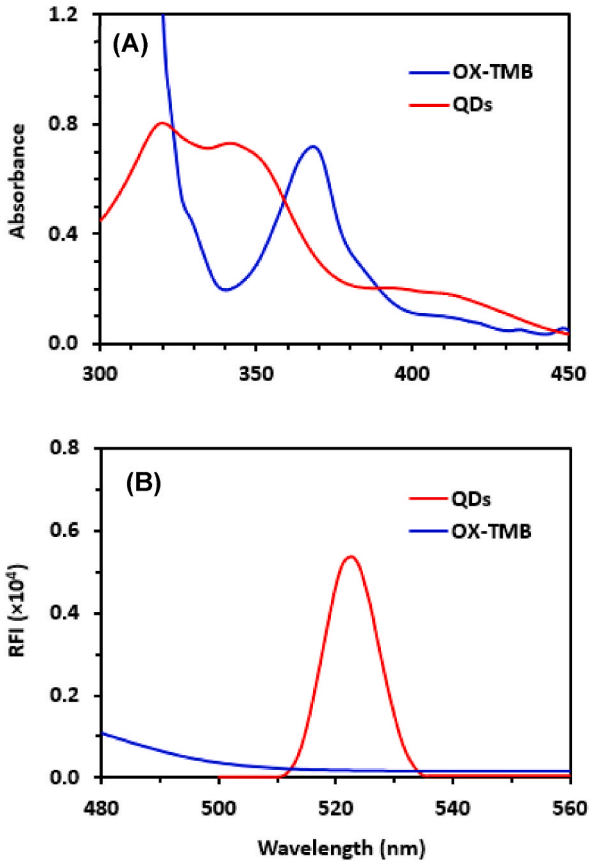

Fig. 2. Absorption (A) and fluorescence emission (B) spectra of QDs and OX-TMB. Emission spectra were recorded using light of 370 nm for excitation.

are required for the IFE-based signal transformation in the detection system [44]. The formation of a quinoid structure with a planar configuration in the excited state and the observed resonance of the OX-TMB molecules (Fig. 3) indicated that they have no influence on the fluorescent outputs of QDs (Fig. 3B), as shown by the absence of fluorescence emission due to OX-TMB at the maximum emission peak of QDs at 525 (Fig. 2B). These findings supported our strategy to employ the IFE of HRP/TMB reaction on the fluorescence of QDs in the development of IFE-FIA described herein.

3.3. Optimization of assay conditions

3.3.1. Selection of CLDN 18.2 concentration for coating the assay plates

Because the IFE-FIA involved the non-competitive binding of ZOL to the CLDN 18.2 protein that has been coated onto the assay plates, it was necessary to have an excess of coated CLDN 18.2 to capture all ZOL molecules in the sample solution. Therefore, a high concentration of ZOL (2 μg/mL) was used to determine the optimal concentration of CLDN 18.2 required for coating onto the assay plate wells. Variable concentrations (0.2–2 μg/mL) of CLDN 18.2 were coated onto the plates, the analysis was conducted, and the fluorescence signal differences (ΔF) were measured. The saturating concentration of CLDN 18.2 was found to be $\geq$ 0.75 μg/mL (Fig. 4A). To ensure an excess of CLDN 18.2, a higher concentration (1 μg/mL) was used for coating in all the subsequent experiments.

3.3.2. Coating conditions of CLDN 18.2

The optimal coating of proteins onto the binding immunoassay plates is greatly affected by the pH and type of buffer solution, temperature, and time of coating. To select the most appropriate buffer for coating CLDN 18.2, different buffer solutions were tested. These buffer solutions were phosphate buffer (PB: pH 7.4), phosphate-buffered saline (PBS: pH 7.4), carbonate buffer (CB: pH 9.6), and hydroxyethylpiperazine ethane sulfonic acid buffer (HEPES: pH 7.0). These buffers were chosen based on their recommendations for coating different proteins in the development of immunoassays [45]. The results demonstrated that the optimal coating of CLDN 18.2 was achieved when CB (pH 9.6) was used (Fig. 4B). The better performance of CB because it promotes the protein solubility and ensures a negative charge, facilitating its binding to positively charged assay plates.

To determine the optimal temperature and incubation time for coating CLDN 18.2, 50 μL of CLDN 18.2 solution (1 μg/mL) was introduced to each well of an assay plate, and the plates were incubated under different conditions: at 4 °C for 12 h, at room temperature (25 °C) for 2 h, and at 37 °C for 2 h. Subsequently, the plates were manipulated as usual. It was found that the optimum coating of CLDN 18.2 occurred when the plates were incubated at 37 °C for 2 h (Fig. 4C). Moreover, the incubation time required for coating at 37 °C was studied by varying the time in the range of 0.5–4 h. A subsequent experiment revealed that an incubation time of 2 h was sufficient for optimal coating (Fig. 4D).

3.3.3. Blocking of assay plate wells

After coating the plate wells with CLDN 18.2, the unoccupied protein binding sites on the well surface should be blocked with a suitable blocking reagent. The selection of a blocker is crucial for achieving a high signal-to-background ratio, which measures the size of the signal obtained with the target analyte compared to the background signal obtained without the target analyte. The ideal blocker should reduce the background signal and enhance the analyte signal, thus improving the sensitivity of the assay. To select the most appropriate blocking agent, 5 different agents were tested: bovine serum albumin (BSA), human serum albumin (HSA), keyhole limpet

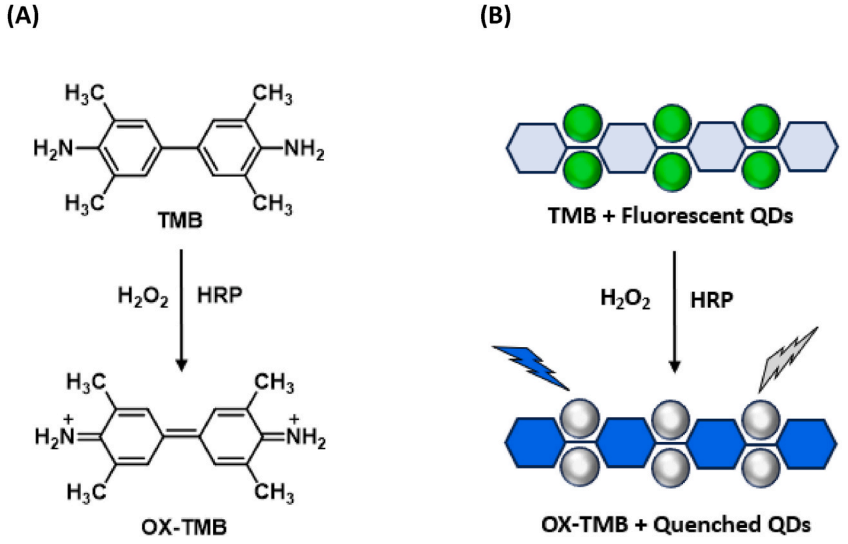

Fig. 3. Panel (A): the mechanism of HRP-calatalyzed oxidation of colorless TMB producing the colored quinonoid structure of OX-TMB. Panel (B): A schematic illustration of quenching of QDs fluorescence by the IFE on the chromogenic HRP-catalyzed oxidation of TMB.

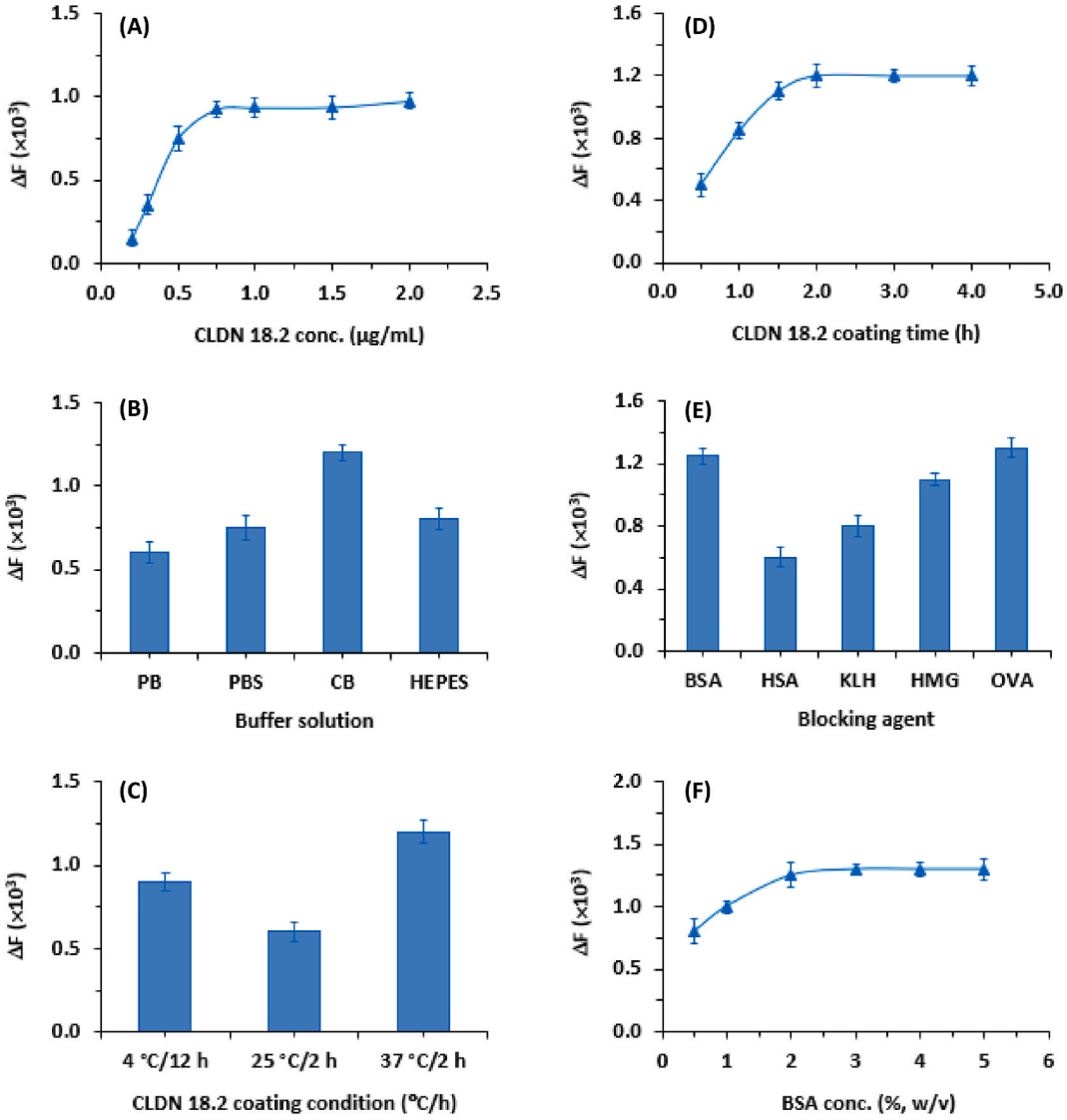

Fig. 4. The results of optimization of conditions for coating and blocking of the IFE-FIA plate wells. (A) the titration of varying concentrations of CLDN 18.2 protein versus a fixed high concentration of ZOL (2 μg/mL). (B) the effect of type of buffer solution on coating efficiency of CLDN 18.2 onto the assay plate wells. (C) the effect of temperature and time on the coating efficiency of CLDN 18.2 onto the assay plate well. (D) the effect of time required for efficient coating of CLDN 18.2 onto the assay plate wells at 37 °C. (E) the effect of the type of blocking agent on blocking of the assay plate wells coated with CLDN 18.2. (F) the effect of time on the blocking efficiency of the assay plate wells with BSA solution (2 %, w/v). The presented values are means of 3 determinations ± SD.

hemocyanin (KLH), human hemoglobin (HMG), and ovalbumin (OVA). The results indicated that BSA and OVA were comparably better than the other blocking agents (Fig. 4E). BSA was selected for the subsequent experiments.

To determine the optimal concentration of BSA required for blocking all the available unoccupied binding sites on the well surface, 100 μL of BSA solution at varying concentrations (0.5–5 % w/v, prepared in PBS of pH 7.4) was added to each well of the assay plate, and the plates were incubated at 37 °C for 1 h. The results revealed that the best blocking efficiency was achieved with BSA concentrations ranging from 2 % to 5 %, w/v (Fig. 4F). A concentration of 2 % (w/v) was used for the subsequent experiments.

3.3.4. Lifespan of coated CLDN 18.2

Considering the clinical application of the proposed IFE-FIA for bioanalysis of ZOL samples, it was important to develop a convenient procedure with a reduced overall analysis time. The lifespan of the assay plates coated with CLDN 18.2 was assessed. After coating the plates with CLDN 18.2 and their blocking, the coated-blocked plates were stored for different durations at 4 °C and −20 °C. Subsequently, the plates were analyzed to determine the remaining reactive amounts of CLDN 18.2 after storage. The results indicated that the coated plates could be stored for up to 6 weeks at either 4 °C or −20 °C without any noticeable deterioration of coated CLDN

18.2 (Fig. 5A). This finding is advantageous because it allows the storage of coated-blocked plates until when the analysis is needed, thereby reducing the overall IFE-FIA time for ZOL by approximately 3 h (2 h for coating and 1 h for blocking).

3.3.5. Concentration and binding conditions of HRP-IgG

To select the optimal concentration of HRP-IgG for binding the CLDN 18.2-ZOL complex onto the plate well, various concentrations (0.1–2 μg/mL) of HRP-IgG were tested. The highest signals were observed when HRP-IgG concentration was 0.5 μg/mL (Fig. 5B). Furthermore, an incubation time of 1 h at 37 °C was found to be sufficient for optimum binding of HRP-IgG and yielded satisfactory signals.

3.3.6. IFE-based fluorescence quenching

The efficiency of IFE is affected by the concentration of QDs and solution conditions in terms of TMB and H_2O_2 concentrations in the solution and its pH. In this study, a commercially available TMB solution for ELISA was used. To select the most appropriate concentration of QDs for mixing with TMB solution, various concentrations (5–40 %, v/v) were tested. The results revealed that the optimum concentration QDs was 20 %, v/v) (Fig. 5C), thus this concentration was used for all the subsequent experiments.

In a subsequent experiment, the time profile of the QDs fluorescence quenching by IFE on HRP/TMB reaction was assessed by monitoring the fluorescence over a period of 30 min. It was found that 15 min was adequate for effective quenching of QDs fluorescence by HRP/TMB reaction (Fig. 5D).

Table 1 provides a summary of the optimal conditions for the proposed IFE-FIA.

3.4. Validation of IFE-FIA

3.4.1. Calibration curve and working range

Under the established optimum conditions of the proposed IFE-FIA (Table 1), the calibration curve for the quantitation of ZOL was generated by plotting the fluorescence inhibition (ΔF, %) as a function of the corresponding concentration of ZOL (Fig. 6A). The working range of the assay was found to 10–400 ng/mL at which 10 and 90 % of the signals were obtained, respectively. Accordingly, the LLOQ and ULOQ were 10 and 400 ng/mL, respectively.

3.4.2. Accuracy and precision

The intra- and inter-assay accuracy and precision of the IFE-FIA were determined at 3 varying concentration levels (25, 100, and

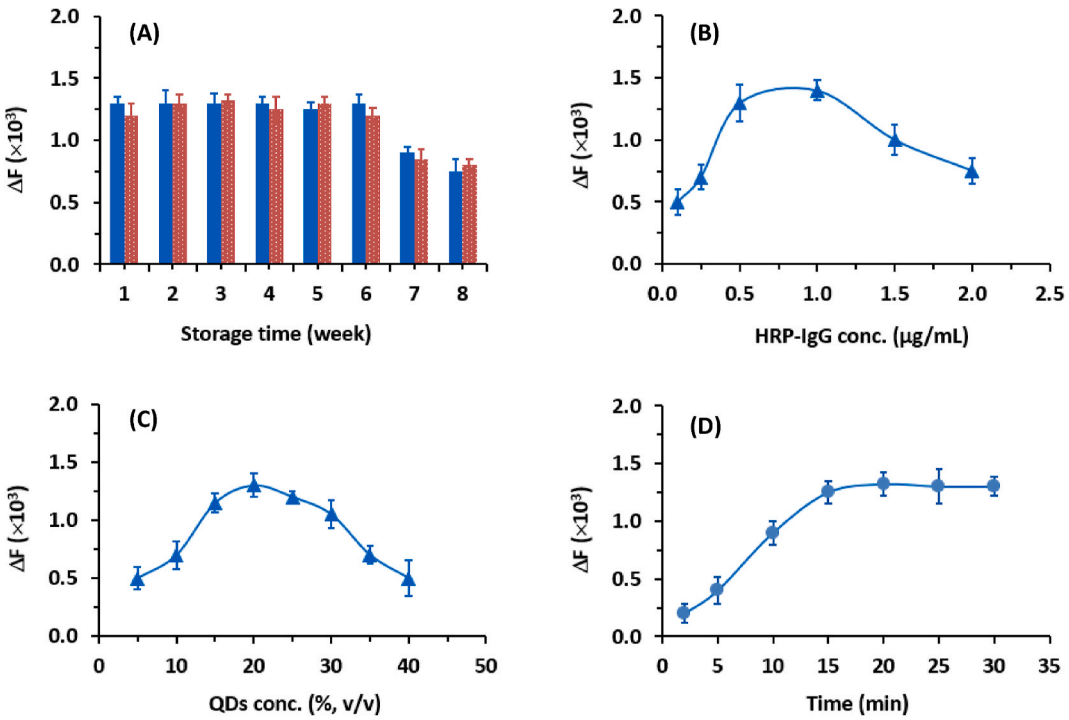

Fig. 5. (A) the life span of CLDN 18.2 that has been coated onto the assay plate wells after storage at 4 °C (solid bars) and at −20 °C (dotted bars). (B) the effect of HRP-IgG concentration required for binding to the CLDN 18.2-ZOL complex. (C) the effect of QDs concentration required for efficient IFE on the HRP/TMB reaction. (D) the fluorescence-time profile of the IFE of QDs on the HRP/TMB reaction. The presented values are means of 3 determinations ± SD.

Table 1
Summary for optimum conditions of IFE-FIA for ZOL.

Parameter/condition	Optimum value
Concentration of CLDN 18.2 for coating (μg/mL)	1
Coating of CLDN 18.2: time (h)/temperature (°C)	2/37
Concentration of BSA for blocking (%, w/v)	2
Blocking with BSA: time (h)/temperature (°C)	1/37
Binding of ZOL: time (h)/temperature (°C)	1/37
Concentration of HRP-IgG (μg/mL)	0.5
Binding of HRP-IgG: time (h)/temperature (°C)	1/37
Fluorescence inhibition by IFE: time (min)/temperature (°C)	15/37
Measuring wavelength (excitation/emission, nm)	340/525

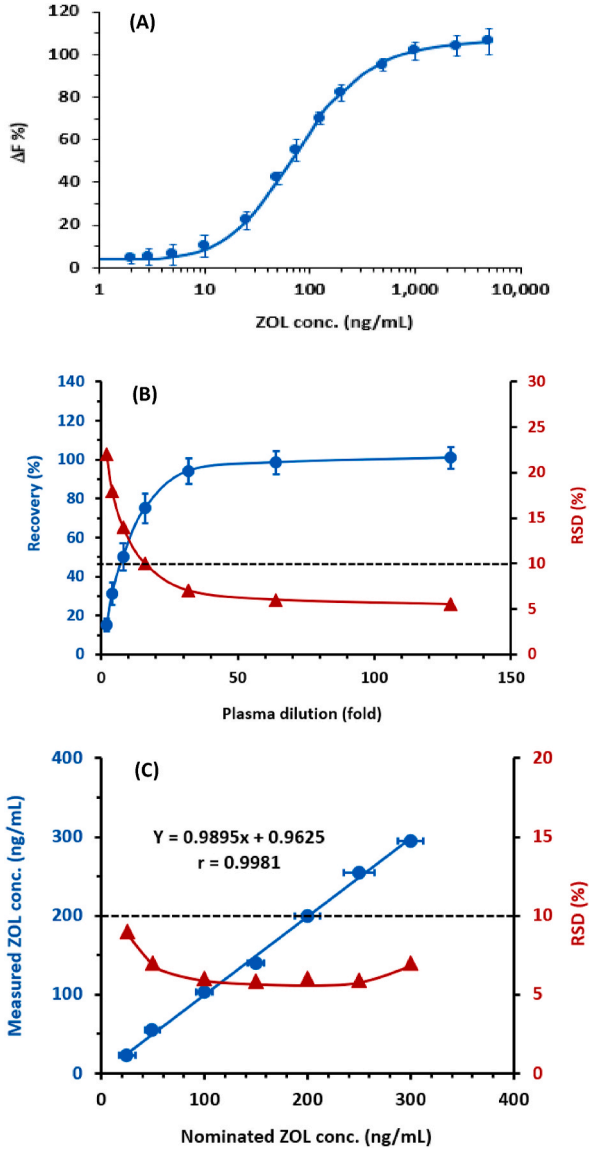

Fig. 6. (A) the calibration curve of the proposed IFE-FIA for ZOL. (B) the effect of plasma matrix on analytical recovery (●) and RSD values (▲) of the quantitation of ZOL in plasma by IFE-FIA. (C) the correlation between the measured concentrations of ZOL with those of spiked nominated concentrations (●) and RSD values (▲) obtained by the proposed IFE-FIA. The presented values are means of 3 determinations ± SD.

250 ng/mL) as described in the experimental section. The accuracy, represented as recovery percentage, was in the range of 96.8–104.5 % (Table 2). The precision, represented as RSD values, was in the range of 4.1–6.2 % and 5.4–6.5 % for intra- and inter-assay precision, respectively. The obtained recovery percentages and RSD values reveal the acceptable according to the guidelines of validation of immunoassays [46].

3.4.3. Effect of plasma matrix and applicability

Since the proposed IFE-FIA was devoted to the quantitation of ZOL in plasma samples, it was necessary to assess the effect of the plasma matrix on the reliability of the assay for applications to real analysis in clinical settings. Drug-free plasma samples were separately spiked with ZOL (400 ng/mL), serially diluted with PBS, and analyzed by IFE-FIA. The dilutions were in the range of 2–128 folds. As shown in Fig. 6B, the recovery values increased as the plasma dilution increased up to 28-fold. At and beyond this dilution, the recovery values reached to ~100 %. Additionally, the RSD values decreased with the dilution increase. The low recovery values and low precision (high RSD values) at low plasma dilutions were attributed to the influence of mass transport and mobility limitations typically observed in immune binding in viscous samples [47–49]. Based on these findings and to avoid false-positive results, it is recommended to dilute plasma samples with PBS at a minimum ratio of 28-fold before conducting the analysis. It should be noted that the proposed IFE-FIA has an extremely high sensitivity at the picogram level, allowing for the dilution of clinical plasma specimens by several thousand-fold to achieve ZOL concentrations within the assay's working range. This was based on the reported maximum concentration of ZOL in the plasma of patients receiving ZOL at a dose of 600–1000 mg/kg was in the range of 331–805 μg/mL [19].

3.5. Analysis of ZOL-spiked plasma samples

The proposed IFE-FIA was applied to analyze plasma samples spiked with different concentrations of ZOL, ranging from 20 to 300 ng/mL. The results showed a strong correlation between the measured and nominated spiked concentrations, with a correlation coefficient of 0.9981. Furthermore, the RSD values remained below 10 % across all ZOL concentrations (Fig. 6C). These high correlations and low RSD values demonstrate the accuracy, precision, and effectiveness of the proposed IFE-FIA in quantifying ZOL in human plasma samples. Additionally, the results indicated that there was no interference from endogenous components or the plasma matrix, highlighting the applicability of the assay for ZOL analysis.

It is wise to mention that investigating the impact of interfering antibodies on the assay's performance is crucial for a comprehensive evaluation. However, the inclusion of other interfering antibodies in this study was limited by ethical considerations and available resources. Obtaining real patient samples with a variety of interfering antibodies requires specific ethical approvals and access to a diverse patient cohort receiving these antibodies. Currently, we are actively working to obtain the required ethical approvals and expand our research to evaluate the performance of our IFE-FIA assay in the presence of various interfering antibodies.

3.6. Advantages of IFE-FIA

The proposed IFE-FIA offers several advantageous features, summarized as follows. Firstly, it utilizes QDs as a fluorescent probe to high sensitivity that allows for accurate quantitation of ZOL even at concentrations as low as 10 ng/mL. Secondly, the assay based on the IFE of QDs on HRP/TMB enzymatic reaction, avoiding the direct chemical labelling of detection reagents which might cause loss of immunoreactivity. Thirdly, the IFE-FIA demonstrated excellent selectivity, ensuring specific measurement of ZOL in plasma without interference from other components or the plasma matrix. This specificity guarantees the reliability and accuracy of the assay results. Fourthly, the IFE-FIA has high-throughput, enabling the simultaneous analysis of multiple samples in clinical laboratories. Finally, the IFE-FIA method eliminates the need for labor-intensive and time-consuming extraction or clean-up procedures for plasma sample preparation prior to analysis, simplifying the workflow and reducing the overall analysis time, thus making it more convenient for laboratory personnel.

In recent years, a class of film-like QDs has been reported and demonstrated superior fluorescence performance [50,51]. These film-like QDs will be investigated in future work for their suitability for the proposed IFE-FIA and other assays in our laboratory.

4. Conclusions

This study aimed to establish an optimized fluorescent immunoassay for bioanalysis of ZOL based on the IFE of QDs on the enzymatic reaction of HRP and TMB substrate. The validation of the assay confirmed its accuracy and precision, rendering it suitable for quantifying ZOL in plasma samples. The assay exhibited high sensitivity and selectivity, allowing for precise quantification of ZOL even at concentrations as low as 10 ng/mL. This high sensitivity has the advantage of requiring only a small volume of plasma samples for analysis, ensuring patient comfort during pharmacokinetic studies, therapeutic drug monitoring, and refining safety profile. The practical convenience of the assay is noteworthy as it can be easily performed in a standard 96-well assay plate using a microplate reader, which is a common instrument in most clinical laboratories. Furthermore, the assay has high throughput capability, enabling the analysis of a batch of hundreds of samples, in triplicate, per day by an analyst. Overall, the proposed IFE-FIA for bioanalysis of ZOL is expected to make significant contributions to the further studies required for refining ZOL therapeutic benefits.

Data availability statement

Data included in article/supp. Material/referenced in article.

Table 2
The accuracy and precision of the proposed IFE-FIA for ZOL at different concentration levels.

ZOL concentration (ng/mL)	Recovery (% ± RSD)	
	Intra-assay	Inter-assay
20	102.4 ± 5.4[a]	103.4 ± 6.2
100	98.2 ± 4.1	101.2 ± 5.4
250	104.5 ± 6.2	96.8 ± 6.5

[a] The values are means of 3 determinations.

CRediT authorship contribution statement

Ibrahim A. Darwish: Writing – review & editing, Writing – original draft, Resources, Project administration, Methodology, Funding acquisition, Conceptualization. **Daohong Zhang:** Writing – review & editing, Supervision, Methodology, Conceptualization. **Mohammed S. Alsalhi:** Writing – review & editing, Writing – original draft, Validation, Investigation, Formal analysis, Data curation, Conceptualization.

Declaration of competing interest

The authors declare that they have no known competing financial interests or personal relationships that could have appeared to influence the work reported in this paper.

Acknowledgments

The authors extend their appreciation to the Researchers Supporting Project Number (RSPD2024R944), King Saud University, Riyadh, Saudi Arabia, for funding this research work.

References

[1] E. Van Cutsem, V.M. Moiseyenko, S. Tjulandin, A. Majlis, M. Constenla, C. Boni, et al., Phase III study of docetaxel and cisplatin plus fluorouracil compared with cisplatin and fluorouracil as first-line therapy for advanced gastric cancer: a report of the V325 Study Group, J. Clin. Oncol. 24 (2006) 4991–4997.
[2] S.E. Al-Batran, J.T. Hartmann, S. Probst, H. Schmalenberg, S. Hollerbach, R. Hofheinz, et al., Phase III trial in metastatic gastroesophageal adenocarcinoma with fluorouracil, leucovorin plus either oxaliplatin or cisplatin: a study of the Arbeitsgemeinschaft Internistische Onkologie, J. Clin. Oncol. 26 (2008) 1435–1442.
[3] Y.K. Kang, W.K. Kang, D.B. Shin, J. Chen, J. Xiong, J. Wang, et al., Capecitabine/cisplatin versus 5-fluorouracil/cisplatin as first-line therapy in patients with advanced gastric cancer: a randomised phase III noninferiority trial, Ann. Oncol. 20 (2009) 666–673.
[4] Y.J. Bang, E. Van Cutsem, A. Feyereislova, H.C. Chung, L. Shen, A. Sawaki, et al., Trastuzumab in combination with chemotherapy versus chemotherapy alone for treatment of HER2-positive advanced gastric or gastro-oesophageal junction cancer (ToGA): a phase 3, open-label, randomised controlled trial, Lancet 376 (2010) 687–697.
[5] Y.Y. Janjigian, K. Shitara, M. Moehler, M. Garrido, P. Salman, L. Shen, et al., First-line nivolumab plus chemotherapy versus chemotherapy alone for advanced gastric, gastrooesophageal junction, and oesophageal adenocarcinoma (CheckMate 649): a randomised, open-label, phase 3 trial, Lancet 398 (2021) 27–40.
[6] J.J. Zhao, D.W.T. Yap, Y.H. Chan, B.K.J. Tan, C.B. Teo, N.L. Syn, et al., Low programmed death-ligand 1-expressing subgroup outcomes of first-line immune checkpoint inhibitors in gastric or esophageal adenocarcinoma, J. Clin. Oncol. 40 (2022) 392–402.
[7] T. Xie, Z. Zhang, X. Zhang, C. Qi, L. Shen, Z. Peng, Appropriate PD-L1 cutoff value for gastric cancer immunotherapy: a systematic review and meta-analysis, Front. Oncol. 11 (2021) 646355.
[8] K. Turksen, Claudins and cancer stem cells, Stem Cell Rev. Rep. 7 (2011) 797–798.
[9] K. Shin, V.C. Fogg, B. Margolis, Tight junctions and cell polarity, Annu. Rev. Cell Dev. Biol. 22 (2006) 207–235.
[10] F. Hollande, E.M. Blanc, J.P. Bali, R.H. Whitehead, A. Pelegrin, G.S. Baldwin, et al., HGF regulates tight junctions in new nontumorigenic gastric epithelial cell line, Am. J. Physiol. Gastrointest. Liver Physiol. 280 (2001) G910–G921.
[11] C. Rohde, R. Yamaguchi, S. Mukhina, U. Sahin, K. Itoh, Ö. Türeci, Comparison of Claudin 18.2 expression in primary tumors and lymph node metastases in Japanese patients with gastric adenocarcinoma, Jpn. J. Clin. Oncol. 49 (2019) 870–876.
[12] C. Qi, J. Gong, J. Li, D. Liu, Y. Qin, S. Ge, et al., Claudin18.2-specific CAR T cells in gastrointestinal cancers: phase 1 trial interim results, Nat. Med. 28 (2022) 1189–1198.
[13] U. Sahin, M. Koslowski, K. Dhaene, D. Usener, G. Brandenburg, G. Seitz, et al., Claudin-18 splice variant 2 is a pan-cancer target suitable for therapeutic antibody development, Clin. Cancer Res. 14 (2008) 7624–7634.
[14] A. Pellino, S. Brignola, E. Riello, M. Niero, S. Murgioni, M. Guido, et al., Association of CLDN18 protein expression with clinicopathological features and prognosis in advanced gastric and gastroesophageal junction adenocarcinomas, J. Personalized Med. 11 (2021) 1095.
[15] Z. Wang, Y. Yang, Y. Cui, C. Wang, Z. Lai, Y. Li, et al., Tumor-associated macrophages regulate gastric cancer cell invasion and metastasis through TGFb2/NF-kB/Kindlin-2 axis, Chin. J. Cancer Res. 32 (2022) 72–88.
[16] U. Sahin, M. Schuler, H. Richly, S. Bauer, A. Krilova, T. Dechow, et al., A phase I dose-escalation study of IMAB362 (Zolbetuximab) in patients with advanced gastric and gastro-oesophageal junction cancer, Eur. J. Cancer 100 (2018) 17–26.
[17] Ö. Türeci, R. Mitnacht-Kraus, S. Wöll, T. Yamada, U. Sahin, Characterization of zolbetuximab in pancreatic cancer models, Oncoimmunol 8 (2019) e1523096.
[18] U. Sahin, Ö. Türeci, G. Manikhas, F. Lordick, A. Rusyn, I. Vynnychenko, et al., FAST: a randomised phase II study of zolbetuximab (IMAB362) plus EOX versus EOX alone for first-line treatment of advanced CLDN18.2-positive gastric and gastrooesophageal adenocarcinoma, Ann. Oncol. 32 (2021) 609–619.
[19] K. Shitara, F. Lordick, Y.J. Bang, P. Enzinger, D. Ilson, M.A. Shah, et al., Zolbetuximab plus mFOLFOX6 in patients with CLDN18.2-positive, HER2-negative, untreated, locally advanced unresectable or metastatic gastric or gastro-oesophageal junction adenocarcinoma (SPOTLIGHT): a multicentre, randomised, double-blind, phase 3 trial, Lancet 401 (2023) 1655–1668.
[20] M.A. Shah, K. Shitara, J.A. Ajani, Y.J. Bang, P. Enzinger, D. Ilson, et al., Zolbetuximab plus CAPOX in CLDN18.2-positive gastric or gastroesophageal junction adenocarcinoma: the randomized, phase 3 GLOW trial, Nat. Med. 29 (2023) 2133–2141.
[21] P. Singh, S. Toom, Y. Huang, Anti-claudin 18.2 antibody as new targeted therapy for advanced gastric cancer, J. Hematol. Oncol. 10 (2017) 105.
[22] C.L. Nigro, M. Macagno, D. Sangiolo, L. Bertolaccini, L. Aglietta, M.C. Merlano, NK-mediated antibody-dependent cell-mediated cytotoxicity in solid tumors: biological evidence and clinical perspectives, Ann. Transl. Med. 7 (2019) 105.

[23] D. Dobkowsk, FDA Accepts Application for Zolbetuximab in Gastric, GEJ Cancers. Cure®'s Newsletter, Cure®'s Newsletter. https://www.curetoday.com/view/fda-accepts-application-for-zolbetuximab-in-gastric-gej-cancers. Accessed 21 January. 2024.
[24] K. Shitara, A.A. Kawazoe, A. Hirakawa, Y. Nakanishi, S. Fruki, M. Fukuda, et al., Phase 1 trial of zolbetuximab in Japanese patients with CLDN18.2+ gastric or gastroesophageal junction adenocarcinoma, Cancer Sci. 114 (2023) 1606–1615.
[25] I.A. Darwish, Immunoassay methods and their applications in pharmaceutical analysis: basic methodology and recent advances, Int. J. Biomed. Sci. 2 (2006) 217–235.
[26] I. Suárez, A. Salmerón-García, J. Cabeza, L.F. Capitán-Vallvey, N. Navas, Development and use of specific ELISA methods for quantifying the biological activity of bevacizumab, cetuximab and trastuzumab in stability studies, J. Chromatogr., B: Anal. Technol. Biomed. Life Sci. 1032 (2016) 155–164.
[27] Somru BioScience Inc, Cetuximab (Erbitux®) PK ELISA, Catalog SBA-100-007-015. http://www.deltaclon.com/pdf/somru/SBA-100-007-015.pdf. Accessed 21 January. 2024.
[28] N. Cézé, D. Ternant, F. Piller, D. Degenne, N. Azzopardi, E. Dorval, H. Watier, T. Lecomte, G. Paintaud, An enzyme-linked immunosorbent assay for therapeutic drug monitoring of cetuximab, Ther. Drug Monit. 31 (2009) 597–601.
[29] Acro Biosystems, ELISA assay kit for anti-PD-1 h-mAb in human serum. https://www.acrobiosystems.com/P2507-ELISA-Assay-Kit-for-Anti-PD-1-h-mAb-in-Human-Serum.html. (Accessed 21 January 2024).
[30] M.A. Hamidaddin, H. AlRabiah, I.A. Darwish, Development and validation of generic heterogeneous fluoroimmunoassay for bioanalysis of bevacizumab and cetuximab monoclonal antibodies used for cancer immunotherapy, Talanta 188 (2018) 562–569.
[31] J.C. Bonilla, F. Bozkurt, S. Ansari, N. Sozer, J.L. Kokini, Applications of quantum dots in food science and biology, Trends Food Sci. Technol. 53 (2016) 75–89.
[32] W. Xiao, Y. Ye, N. Li, H. Xu, Y. Lv, R. Wu, H. Shen, L.S. Li, Preparation of 3D pomegranate-like quantum dot nanobeads and its application to highly sensitive detection of aflatoxin B1, Microchem. J. 200 (2024) 110380.
[33] Y. Lv, J. Fan, M. Zhao, R. Wu, L.S. Li, Recent advances in quantum dot-based fluorescence-linked immunosorbent assays, Nanoscale 15 (2023) 5560–5578.
[34] G. Hu, D. Su, Q. Yu, T. Zhao, S. Gao, J. Hao, Sensitive fluorescence immunoassay on the basis of the fluorescence quenching effects of quantum dots for the determination of norfloxacin in animal-origin foods, Food Biosci. 58 (2024) 103681.
[35] L. Xu, F. Yang, A.C. Dias, X. Zhang, Development of quantum dot-linked immunosorbent assay (QLISA) and ELISA for the detection of sunset yellow in foods and beverages, Food Chem. 385 (2022) 132648.
[36] S. Zhan, X. Huang, R. Chen, J. Li, Y. Xiong, Novel fluorescent ELISA for the sensitive detection of zearalenone based on H_2O_2-sensitive quantum dots for signal transduction, Talanta 158 (2016) 51–56.
[37] L. Rios, A.A. Garcia, Dendrimer based non-competitive fluoroimmunoassay for analysis of cortisol, React. Funct. Polym. 68 (2008) 307–314.
[38] I. Hemmil, Fluoroimmunoassays and immunofluorometric assays, Clin. Chem. 31 (1985) 359–370.
[39] S.E. Kakabakos, S. Georgiou, P.S. Petrou, I. Christofidis, Heterogeneous fluoroimmunoassays using fluorescein as label with measurement of the fluorescence signal directly onto the solid-phase, J. Immunol. Methods 222 (1999) 183–187.
[40] F. Si, R. Zou, S. Jiao, X. Qiao, Y. Guo, G. Zhu, Inner filter effect-based homogeneous immunoassay for rapid detection of imidacloprid residue in environmental and food samples, Ecotoxicol. Environ. Saf. 148 (2018) 862–868.
[41] J. Sun, J. Zhao, L. Wang, H. Li, F. Yang, X. Yang, Inner filter effect-based sensor for horseradish peroxidase and its application to fluorescence immunoassay, ACS Sens. 3 (2018) 1.
[42] B. Dong, H. Li, G.M. Mari, X. Yu, W. Yu, K. Wen, Z. Wang, Fluorescence immunoassay based on the inner-filter effect of carbon dots for highly sensitive amantadine detection in foodstuffs, Food Chem. 294 (2019) 347–354.
[43] X. Jiang, F. Geng, Y. Wang, J. Liu, P. Qu, M. Xu, Fluorescence turn-on and colorimetric dual readout assay of glutathione over cysteine based on the fluorescence inner-filter effect of oxidized TMB on TMPyP, Biosens. Bioelectron. 81 (2016) 268–273.
[44] H.C. Chang, J.A. Ho, Gold nanocluster-assisted fluorescent detection for hydrogen peroxide and cholesterol based on the inner filter effect of gold nanoparticles, Anal. Chem. 87 (2015) 10362–10367.
[45] J. Gibbs, M. Vessels, M. Rothenberg, Optimizing the Immobilization of Protein and Other Biomolecules for ELISA Assays Application Note, Corning Incorporated Life Sciences. https://www.corning.com/catalog/cls/documents/application-notes/CLS-DD-AN-455.pdf. Accessed 21 January. 2024.
[46] J.W.A. Findlay, W.C. Smith, J.W. Lee, G.D. Nordblom, I. Das, B.S. DeSilva, M.N. Khan, R.R. Bowsher, Validation of immunoassays for bioanalysis: a pharmaceutical industry perspective, J. Pharm. Biomed. Anal. 21 (2000) 1249–1273.
[47] W. Kusnezow, Y.V. Syagailo, S. Ruffer, K. Klenin, W. Sebald, J.D. Hoheisel, C. Gauer, I. Goychuk, Kinetics of antigen binding to antibody microspots: strong limitation by mass transport to the surface, Proteomics 6 (2006) 794–803.
[48] W. Kusnezow, Y.V. Syagailo, I. Goychuk, J.D. Hoheisel, D.G. Wild, Antibody microarrays: the crucial impact of mass transport on assay kinetics and sensitivity, Expert Rev. Mol. Diagn. 6 (2006) 111–124.
[49] K.V. Klenin, W. Kusnezow, J. Langowski, Kinetics of protein binding in solid-phase immunoassays: theory, J. Chem. Phys. 122 (2005) 214715.
[50] S. Zheng, X. Xia, B. Tian, C. Xu, T. Zhang, S. Wang, C. Wang, B. Gu, Dual-color MoS2@QD nanosheets mediated dual-mode lateral flow immunoassay for flexible and ultrasensitive detection of multiple drug residues, Sensor. Actuator. B Chem. 403 (2024) 135142.
[51] C. Wang, Q. Yu, J. Li, S. Zheng, S. Wang, B. Gu, Colorimetric–fluorescent dual-signal enhancement immunochromatographic assay based on molybdenum disulfide-supported quantum dot nanosheets for the point-of-care testing of monkeypox virus, Chem. Eng. J. 472 (2023) 144889.